Nuclear Materials and Energy 42 (2025) 101872

Contents lists available at ScienceDirect

Nuclear Materials and Energy

journal homepage: www.elsevier.com/locate/nme

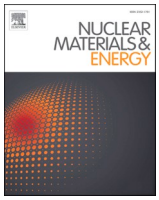

Time dependence of fuel retention in JET be plasma-facing components – Comparison of single and multiple ITER-like wall campaigns

Y. Zayachuk [a,*], N. Catarino [b], J. Likonen [c], M. Rubel [d,e], A. Widdowson [a], JET contributors[1]

[a] UK Atomic Energy Authority, Culham Campus, Abingdon, OX14 3DB Oxfordshire, UK
[b] IPFN, Instituto Superior Técnico, Universidade de Lisboa, 1049-001, Lisboa, Portugal
[c] VTT Technical Research Centre of Finland, PO Box 1000, FIN-02044 VTT, Finland
[d] KTH Royal Institute of Technology, Fusion Plasma Physics, 100 44 Stockholm, Sweden
[e] Uppsala University, Department of Physics and Astronomy, 751 20 Uppsala, Sweden

ARTICLE INFO

Keywords:
JET ITER-like wall
TDS
IBA
SIMS
Hydrogen retention
Beryllium

ABSTRACT

Deuterium retention was measured in beryllium samples from the JET ITER-like wall limiter tiles that were in the JET vessel for one and three campaigns (in vessel during 2015–2016 and 2011–2016, respectively), using thermal desorption spectroscopy, ion beam analysis and secondary ion mass spectrometry. It was found that overall retention increases with time non-linearly but somewhat slower than a square root of plasma exposure time. Depth distribution of retained deuterium was observed to change with time, with near-surface content being variable and dependent on recent plasma exposure conditions, and bulk contribution progressively increasing. Desorption peaks were observed to shift to higher temperatures with time. Experimental evidence suggests that long-term deuterium accumulation in the Be limiter components in JET is diffusion-dominated, with observed changes as function of time being consistent with the correspondingly deeper diffusion due to the propagation of the diffusion front. Cleaning interventions are found to only slow down this propagation and not stop it.

1. Introduction

Between 2011 and the end of its operations in 2023, JET tokamak operated with ITER-like wall (ILW), with its plasma-facing components (PFCs) consisting predominantly of bulk W and W-coated CFC tiles in the divertor and bulk Be tiles in the main chamber, where these Be tiles form discrete poloidal limiters [1–3]. JET operations with ILW were organized in discrete campaigns, with shutdowns in between [4]. During these shutdowns in-vessel work was performed which included removal of in-vessel components including PFCs, which then were used for subsequent plasma-wall interaction (PWI) studies, including ex-situ measurements of fuel retention [5–16]. Campaigns that were associated with component removal include ILW1 (2011–2012, component removal in 2012), ILW2 (2013–2014, component removal in 2014) and ILW3 (2015–2016, component removal in 2016). The shutdown in 2016 was so far the latest in which components were removed, with the follow up expected in 2024.

Previous ex-situ studies of hydrogen isotope retention with ILW focused on retention in PFCs in each individual campaign [17–21]. A defining feature of the ex-situ studies is that they are necessarily performed after the completion of a given campaign and therefore reflect the final result of the entirety of a given campaign. This means that the information on time dependence of retention in the JET environment is lost, since there is no direct experimental evidence of how hydrogen retention was changing as a function of accumulated plasma exposure time. For the operation of a fusion power plant such information is critical, as it is important to understand the long-term effects of exposure of the PFCs to plasma and temporal dynamics of accumulation of hydrogen isotopes in a tokamak environment, both from the perspectives of tritium production and self-sufficiency, and PFC lifetime estimates [23,24]. Component removal performed in 2016 (following the ILW3 campaign) provided an opportunity for such studies. One of the sets of Be limiter tiles removed in 2016 consisted of tiles that were installed during the initial assembly of the ILW and not exchanged since; these tiles were exposed to plasma for the entire duration of three ILW campaigns, 2011–2016 (referred to as ILW1-3). Simultaneously, another

* Corresponding author.
E-mail address: Yevhen.Zayachuk@ukaea.uk (Y. Zayachuk).
[1] *See list of authors: "Overview of T and D-T results in JET with ITER-like wall" by C F Maggi et al., Nuclear Fusion 64 (2024) 112012.*

https://doi.org/10.1016/j.nme.2025.101872
Received 22 August 2024; Received in revised form 2 January 2025; Accepted 8 January 2025
Available online 11 January 2025

set of tiles was removed, but these tiles were only installed during the previous shut-down in 2014, and were only exposed to plasma for the duration of a single ILW campaign, 2015–2016 (ILW3). Therefore, it became possible to compare the retention in the tiles exposed for significantly different amounts of time, ILW1-3 vs ILW3.

Detailed comparison of deuterium (D) content and depth distribution in both sets of tiles is the main objective of this work. Focus is on D (not on tritium) since the investigated samples were removed from JET vessel prior to T and DT campaigns in 2021 and 2023, thus the amount of retained tritium is very low [25,26]. Three complementary measurement techniques were used for D quantification – thermal desorption spectroscopy, ion beam analysis and secondary ion mass spectrometry.

2. Experimental

Samples used for this study were single castellations (or further size-reduced sub-castellations) cut out of bulk Be limiter tiles of JET ILW, removed from JET vessel after the ILW3 campaign in 2016. These castellations have dimensions of 12×12×2 mm, and sub-castellations are quarters of these with the dimensions of ~5.5x5.5x2 mm. Multiple samples from each tile were studied, providing a measurement of distribution of retention across each tile in the toroidal direction – Fig. 1a presents a general overview of one of the tiles indicating castellations used for measurements. Inner wall guard limiter (IWGL) tile 2XR10 and outer wide poloidal limiter (WPL) tile 4D14 were in the JET vessel only for the duration of a single ILW3 campaign (i.e., during 2015–2016), while IWGL tile 2XR11 and WPL tile 4D15 were in the vessel since the beginning of JET operations with ILW, i.e. during three ILW campaigns – 2011–2016. All of these tiles are located close to the mid-plane of the main chamber of JET, as shown in Fig. 1b. Samples from 2XR10 and 4D14 tiles (in vessel 2015–2016) are referred to in the following discussion as ILW3 samples, while those from 2XR11 and 4D15 (in vessel 2011–2016) are referred to as ILW1-3 samples.

Cumulative times of limiter plasmas touching the corresponding tiles, defined as the time during which limiter plasma was within 2 mm of the limiter surfaces are shown in Table 1 (from [18]); the criterion of 2 mm represents an average width of scrape-off layer (SOL) in JET ([22]). Note that in the case of 2XR11 and 4D15, as these tiles were in the JET vessel for the entire duration of three campaigns, the total cumulative time for ILW1-3 is defined as the sum of the durations of these individual campaigns.

Thermal desorption spectroscopy (TDS) was performed using a Hiden Analytical Type 640,100 TPD Workstation at UKAEA, Culham, UK. Details of the facility can be found in [9]. Desorption measurements

Table 1
Cumulative time of limiter plasma on tiles (within 2 mm from limiter surfaces).

Tile	ILW1, hrs	ILW2, hrs	ILW3, hrs	ILW1-3, hrs
2XR10	1.73	1.35	0.80	–
2XR11	2.30	1.92	1.04	5.26
4D14	2.36	1.76	1.77	–
4D15	1.45	0.73	0.67	2.85

were performed at a base pressure of ~2×10^{-9} mbar with a constant heating rate of 10 K/min, up to a maximum nominal temperature of 775 °C and 1 hr hold time at maximum temperature. The heating system is a molybdenum heating plate with a sample placed on it; a protective layer of AlN is placed between the Be sample and the heater to avoid adhesion of the sample to the heater at elevated temperature. This requires the use of a calibration function derived in [27] to determine the true temperature of the sample. Desorbed molecules are detected by a line-of-sight quadrupole mass spectrometer (QMS). Molecular fluxes of masses 3 (HD molecules) and 4 (D_2 molecules) are recorded; they are quantified using calibrated H_2 and D_2 calibrated leaks, with the calibration factor for HD being the average between the factors for H_2 and D_2. The error in determination of retention, based on comparison of the measurements on calibrated lab-produced samples (from [27]), is estimated to be <10 %. 60 K is taken as a general estimate of the maximum uncertainty in determination of the desorption peaks temperatures ([27]). Desorption flux of atomic D, F_D, is calculated as a sum $F_D = F_{HD} + 2F_{D2}$, where F_{HD} and F_{D2} are molecular release fluxes of masses 3 and 4, respectively.

Ion beam analysis (IBA) was performed using a 2.5 MV Van de Graaff accelerator at the Laboratory of Accelerators and Radiation Technologies, Lisbon, Portugal. The accelerator is equipped with a chamber dedicated to fusion research, where Be- and tritium-containing samples can be handled. To determine D concentrations in the investigated samples, Rutherford backscattering (RBS) and nuclear reaction analysis (NRA) were performed using ^{3}He ions at an energy of 2.3 MeV. A particle detector for RBS is located at a scattering angle of 150°. The detector for NRA is placed at a 135° scattering angle. It has an active layer with 2 mm thickness to detect the protons from D(^{3}He,p)^{4}He reaction that have 12.5 MeV energy. A particle filter in front of the NRA detector, with a 140 μm thick Al foil, absorb the scattered primary ions and the 14 MeV α particles from ^{9}Be(^{3}He,α_0)^{8}Be. Deuterium quantification was performed using the NDF code [28], cross sections for D(^{3}He,p)^{4}He reaction are calculated internally by the NDF code, following the expression of Möller and Besenbacher [29]. At the beam energy used the maximum interaction depth for the D concentration analysis from ^{3}He

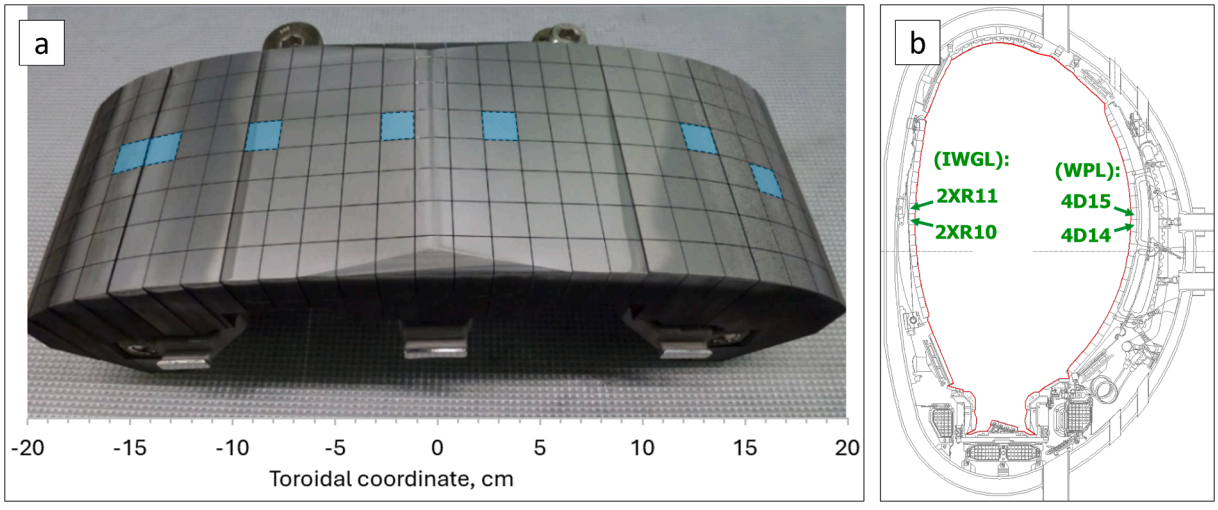

Fig. 1. (a) General appearance of a IWGL tile, with the marked castellations on which TDS measurements were performed; (b) cross-section of JET vessel, showing poloidal locations of the studied tiles.

NRA in Be is 9 μm. The statistical error bars in IBA data are estimated to be less than 10 % for the concentration of 10^{18} at/cm^2 and increase to the order of 50–80 % for the concentration below 10^{15} at/cm^2, due to the very low signal for NRA.

Secondary ion mass spectrometry (SIMS) was performed using a double focusing magnetic sector instrument VG Ionex IX-70S at VTT Technical Research Centre of Finland, Espoo. A 5 keV O_2^+ primary beam with 500nA current was raster-scanned over an area of 300 × 400 μm^2. A 10 % electronic gate was used to avoid crater wall effects. This electronic gate means that secondary ion signal was collected from the centre of the crater with an area of 95×125 μm^2 which is 10 % of the total sputtered area. The intensities of the positive secondary ions at mass to charge ratios (m/q) of 1 (H), 2 (D), 9 (Be), 12 (C) and 58 (Ni) were measured as a function of time. After each measurement, the depth of the crater was measured with a profilometer. The measurement depth was between 9 μm and 50 μm. An ion implanted sample was used to determine the relative sensitivity factor (RSF) for D in Be. This RSF was then used to determine D concentration in the Be samples. The accuracy of the SIMS measurements is typically ~30 %.

3. Results

Fig. 2 shows the distribution of D retention across the tiles in the toroidal direction, as measured by TDS and IBA. Results from ILW3 samples are compared with those from ILW1-3 (IBA and some of the TDS results from ILW3 samples were previously presented in [27], and IBA results from ILW1-3 samples in [18]). It can be seen that overall toroidal the distribution of retention after 3 campaigns follows the same dependence as for an individual campaign – i.e., lower retention in the central part of the tile (corresponding to the erosion-dominated zone where retention is mainly implantation-driven) and higher retention in the periphery of the tiles (i.e., in the deposition-dominated zones where retention is driven by co-deposition with sputtered material, mostly Be).

TDS measurements show that bulk retention after ILW1-3 is systematically higher across the entirety of tiles compared to a single campaign, ILW3. The ratio between retention in ILW1-3 and ILW3 samples for each toroidal position where samples from both sets of tiles are available, has been calculated as ~1.8 for IWGL and ~1.4 for WPL. The average ratio of all such pairs is ~1.6. In contrast to this, the near-surface retention For single campaign, ILW3, and three campaigns, ILW1-3, as measured by IBA, is comparable throughout the tiles, both in erosion and deposition zones.

When comparing retention measured by TDS and by IBA, for ILW3 and ILW1-3 samples, it can be seen that both after single campaign and after three campaigns in the erosion zone retention measured by TDS is systematically, and substantially, higher than measured by IBA, while in the deposition zone TDS results are either comparable or only somewhat higher than those of IBA.

In Fig. 3 D depth distributions measured by SIMS on a pair of samples from ILW3 and ILW1-3 IWGL tiles are shown. Samples on which these measurements were performed were chosen such that their toroidal position within their corresponding tiles, were identical. Positions of these specific samples, −12.6 cm, fall within the deposition zone. It can be seen that the concentrations measured for ILW3 and ILW1-3 samples are essentially identical at the surface, but differ further in depth, with D concentrations in the ILW1-3 sample being higher than in ILW3 sample, with the difference progressively increasing as function of depth.

Fig. 4 presents proton energy spectra from NRA measurements on selected locations within the erosion and deposition zones. The depth scale in the figure corresponds to an approximate estimate of the depth in the sample from where the signal of the corresponding energy channel originates. This depth scale was obtained by simulating D in Be at different depths using NDF [28] and assuming a density of 12.05×10^{22} at/cm^2 and stopping powers from SRIM [30]. While these spectra do not directly represent depth distribution of D content in the samples, comparison of spectra from different samples provides a qualitative measure

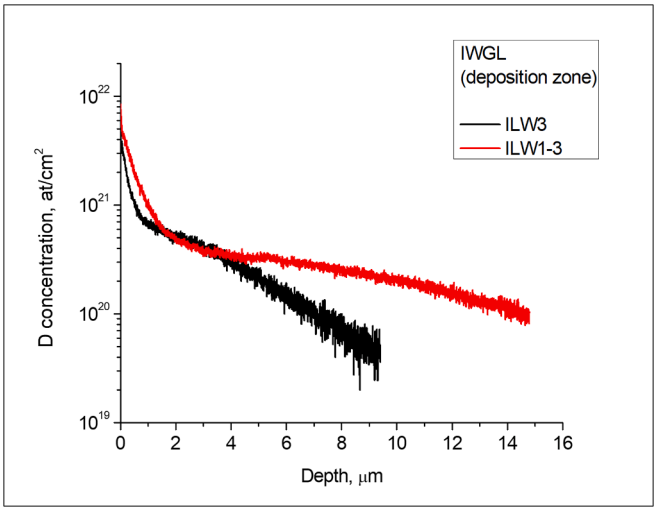

Fig. 3. SIMS depth distributions for samples from the deposition zones of IWGL tiles (ILW3 and ILW1-3).

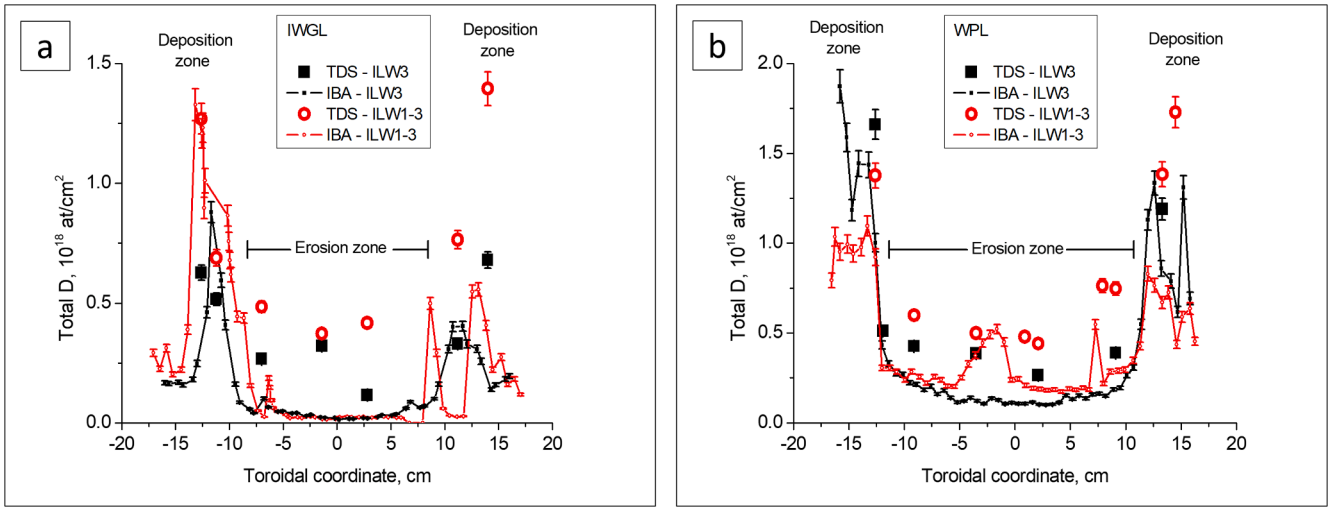

Fig. 2. Toroidal distribution of D retention in the limiter tiles after single and three ILW campaigns, as measured by TDS and IBA: (a) IWGL tiles; (b) WPL tiles.

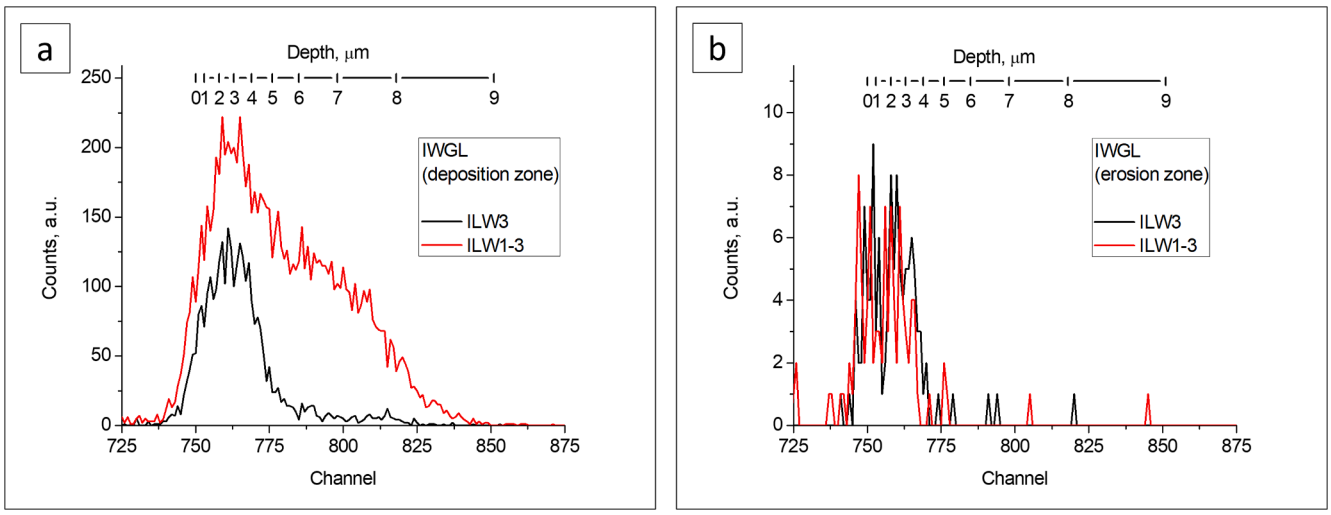

Fig. 4. NRA proton energy spectra showing the D depth distribution (IWGL tiles).

of the difference in such distributions. Particularly in the deposition zone, D content in the depth range beyond ~4 μm from the surface is noticeably higher after ILW1-3 as compared to ILW3. On the other hand, in the erosion zone D depth distributions after ILW1-3 and ILW3 appear to be similar, however overall D content within IBA range is very low in both, and signal intensity is insufficient to directly provide an indication in the difference in D depth distributions.

Fig. 5 presents a comparison of the desorption spectra measured at similar toroidal positions after ILW3 and ILW1-3. Spectra shown here are characteristic examples for the deposition (Fig. 5a) and erosion (Fig. 5b) zones. It is seen that in the deposition zone spectra are similar in shape, with a single clearly defined maximum. At the same time in the erosion zone there is a variation in the shape of the spectra, though even here typically there is a well-defined primary peak – though secondary peaks might be present, with varying intensity relative to the primary peak (secondary peaks in the examples shown in Fig. 5a are denoted by arrows).

A remarkable feature of the difference between single campaign and three campaigns is the fact that in the ILW1-3 samples the primary release maxima are at a systematically higher temperature than in the ILW3 samples. This is evident in the examples in Fig. 5, but this behaviour is characteristic for all the studied pairs of samples, corresponding to the entire toroidal spans of the investigated tiles. Fig. 6 shows the dependence of the temperature of primary release peak as function of toroidal position within a tile. Particularly for IWGL tiles this dependence is very similar in shape for both ILW3 and ILW1-3 tiles, but with an offset, such that values ILW1-3 are systematically higher. Indeed, even specific features of this toroidal dependence, such as e.g. dip at the coordinate around −7.5 cm or maximum around 10 cm, are present in both tiles. For WPL the maxima of release are also systematically higher for ILW1-3 samples compared to ILW3 ones, but subtle features of coordinate dependence are less well reproduced. The average difference between the maxima in ILW3 and ILW1-3 spectra is ~60 °C for IWGL and ~100 °C for WPL.

4. Discussion

The samples investigated in this study were all removed from the JET vessel at the same time and were all exposed to plasma in JET during ILW3. ILW1-3 samples have pre-ILW3 history of exposure which ILW3 samples, by definition, lack. Therefore, the essence of the question that comparison of ILW3 and ILW1-3 samples is addressing is – what is the effect of pre-ILW3 plasma exposure on retention observed at the end of ILW3 campaign? In other words, is retention behaviour in long exposed ILW1-3 samples dominated by the most recent period of exposure (i.e., ILW3) and is therefore equivalent to that in ILW3 samples, or does prior

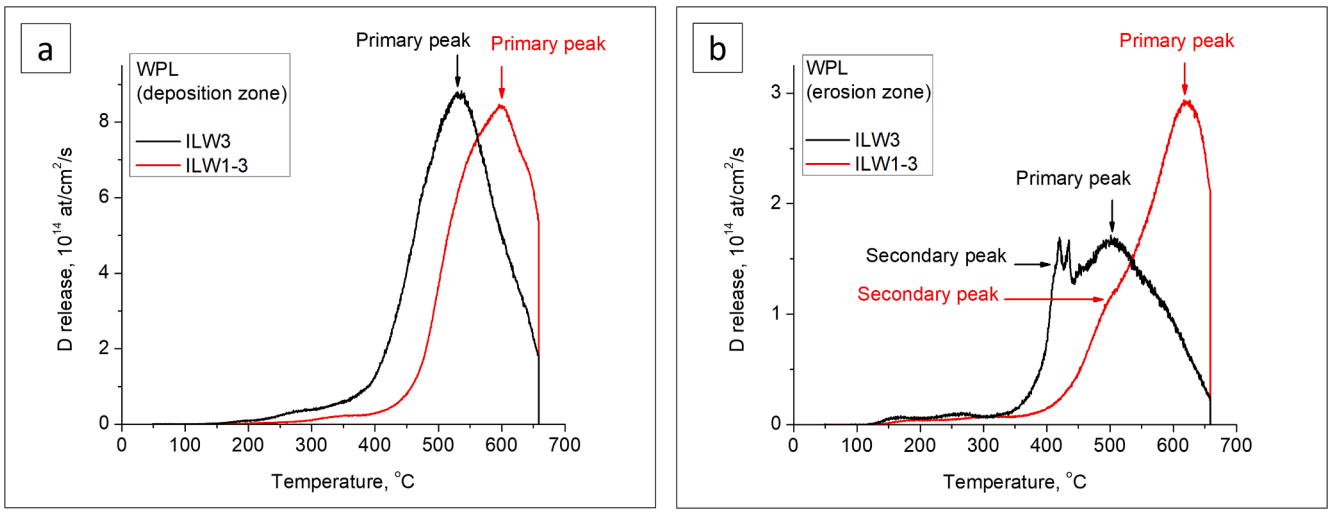

Fig. 5. Characteristic desorption spectra from the WPL samples: a) deposition zone; (b) erosion zone.

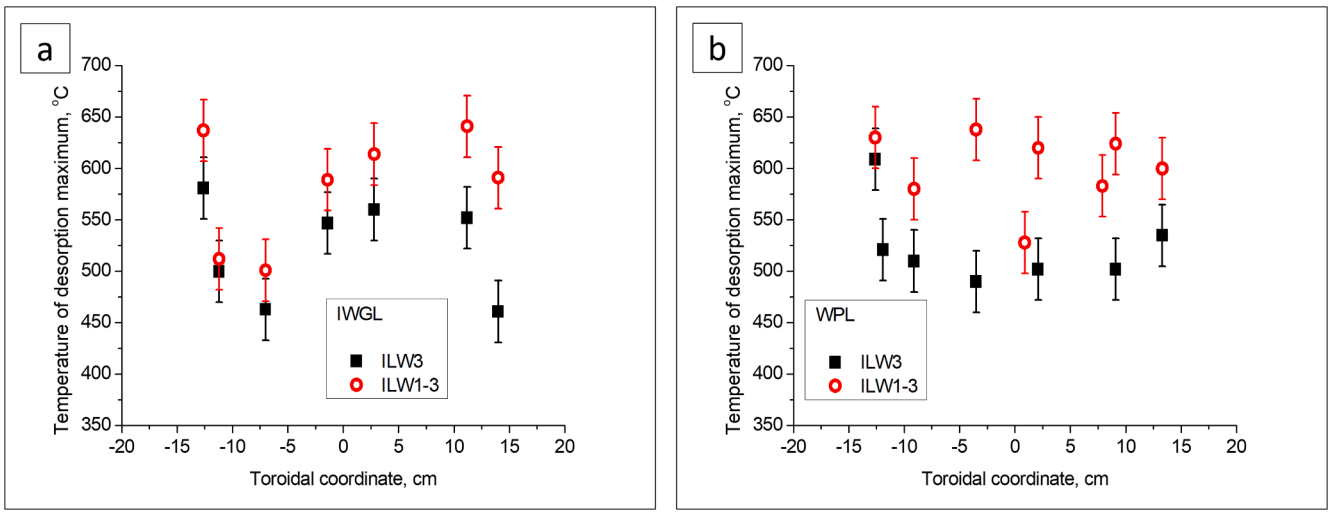

Fig. 6. Temperature maxima of primary desorption peaks plotted against the toroidal positions of the samples: (a) IWGL; (b) WPL.

history – exposure during ILW1 and ILW2 – have a lasting effect, which is not eliminated by the intervening plasma operations?

To compare the cumulative plasma conditions experienced by the investigated samples that were in the vessel during a single campaign and those after three campaigns, it is informative to consider the overall time their original tiles were exposed to plasma during each campaign. As limiter tiles are in contact with the plasma during the limiter phase of an individual JET pulse, and this is when majority of ion flux is accumulated on them, the comparison of the limiter phase times, presented in Table 1, would be the most informative one, albeit with certain limitations discussed below.

Comparison of plasma exposure times only during the last campaign, ILW3 shows that the IWGL tile that was in the vessel for ILW1-3 campaigns, 2XR11, was in contact with limiter plasma for ~0.8 h, and the tile that was in the vessel for only ILW3 campaign, 2XR10, was in contact with limiter plasma for ~1 h, corresponding to a factor of difference of ~1.25. Compare this to the factor of difference in retention of ~1.8. In the case of WPL the factor of difference in limiter plasma contact time during ILW3 is ~0.38 (with ILW1-3 tile 4D15 in contact with limiter plasma for 0.67 hrs and ILW3 tile 4D14 for 1.77 hrs) while the factor of difference in retention is ~1.4. It is evident that the increase in retention in ILW1-3 tiles compared to their ILW3 counterparts is not correlated with the difference in plasma contact time during ILW3, but instead systematically exceeds it. This suggests that values of retention observed in ILW1-3 samples are not determined exclusively by the exposure during latest (ILW3) campaign, and the influence of a prior history of plasma exposures is observed.

On the other hand, comparison of the entire cumulative plasma exposure times accumulated by the samples in the vessel, can be done. In the case of IWGL, ILW1-3 tile 2XR11 was exposed to a total of ~5.3 h of limiter phase time throughout three campaigns, as compared to 0.8 h for the ILW3 tile 2XR10. I.e., cumulative duration of the limiter phase over three campaigns is a factor of ~6.6 larger than during the single ILW3 campaign, compared to the factor of difference in retention of 1.8. In the case of WPL, ILW1-3 tile 4D15 was exposed to 2.8 h of limiter plasma time, while ILW3 tile 4D14 to 1.8 h, with a factor of difference ~1.6 difference, compared to the factor of difference in retention of ~1.4. Therefore, it can be seen that total retention as function of total cumulative plasma exposure time scales slower than linearly.

It should be noted that the difference in retention between ILW3 and ILW1-3 tiles might not be fully captured by the comparison of corresponding limiter plasma times, and influenced by other factors, that are difficult to quantify. In particular, the retention dynamics can be impacted by the tile temperature during a JET plasma pulse. ILW3 and ILW1-3 tiles were in neighbouring but not identical poloidal positions within the same limiter beams (see Fig. 1b), and therefore their temperature during the campaigns would not be identical either. Unlike exposure time, which can be presented as a single cumulative number characterizing each ILW campaign, temperature is both spatially and temporarily non-uniform, changing within an individual pulse and from pulse to pulse. Full integration of IR cameras heat flux data was not possible within the scope of this study. On the other hand, this non-uniformity in heat flux reflects the non-uniformity of ion flux arriving at the limiters. The information on ion fluxes on individual tiles was not available for the entire campaigns, and therefore a direct calculation of accumulated ion fluences was not possible. In addition, the information on charge-exchange fluxes for the entire campaigns and their corresponding campaign-integrated fluences was not available either. However, despite these limitations, a qualitative assessment can be given. The main plasma-limiter interaction occurs at the midplane tiles, namely tile 2XR11 on the inner wall (which was an ILW1-3 tile) and 4D14 on the outer wall (ILW3 tile), and this is where the maximum heat and ion fluxes and maximum overall temperature can be expected [31,18]. Other tiles used for comparison, namely 2XR10 (ILW3) and 4D14 (ILW1-3) were somewhat removed from these areas of maximum heat flux, and thus would generally have lower temperatures and ion fluxes. Therefore, in the case of IWGL, the temperature and ion flux are expected to be higher in ILW1-3 tile compared to ILW3 one, but in the case of WPL it is the opposite, and temperature and ion flux are expected to be lower in ILW1-3 tile, compared to ILW3 one. Despite these opposite relative dynamics, the increase of retention is observed for both IWGL and WPL pairs of tiles. Thus, it can be concluded that the differences in temperature and ion flux have a minor effect on the qualitative retention behaviour (although quantitatively it can influence measured retention ratios).

Results from the two main techniques used in this study – NRA and TDS – demonstrate somewhat different changes in measured values of D content between ILW3 and ILW1-3 samples. As seen in Fig. 2, values of retention measured by NRA are similar between ILW1-3 and ILW3 samples; at the same time, values of retention as measured by TDS are systematically higher in ILW1-3 samples compared to ILW3 ones. IBA provides measurements of retention in the near-surface region within its range, while TDS is sensitive to the bulk retention. These results suggest that D accumulation as a function of time progresses differently in the near-surface region and in the bulk. The near-surface D content appears not to be influenced by a prior history of plasma exposure to a significant degree and instead reflects only recent exposure conditions. Additional evidence for this interpretation of the similarity if the near-surface

content, as opposed to near-surface content reaching certain steady state as a result of cumulative plasma exposure, can be found in the IBA data on retention in Be limiter tiles after individual ILW campaigns published in [18] (Fig. 3 therein). They show that the values of retention are noticeably different from campaign to campaign, which is particularly noticeable in the case of ILW2 data. ILW2 finished with a number of protium plasma pulses which removed a considerable amount of near-surface D via isotope exchange. Thus, it can be inferred that near-surface D content can change considerably as function of recent history, and therefore the fact that it is similar for ILW3 and ILW1-3 samples means that D content observed in this case is a reflection of accumulation during ILW3, with prior history of exposure having no discernible effect. On the other hand, increase in the retention values measured by TDS indicates that bulk D content increases as a result of such history, and consequently, the overall increase in retention with time, described above, occurs due to the increase of this bulk content.

To understand the dynamics of D accumulation as a function of time, it is useful to compare retention as measured by TDS and IBA for a given set of samples, and to analyse how this difference changes between ILW3 and ILW1-3. Such comparison between the TDS and IBA results reflects the changes in the depth distribution of D and allows observing the difference between the near-surface and bulk dynamics of D accumulation. Near-surface is defined as the depth within IBA sampling range, and bulk as depth beyond this range. As a quantitative measure of the relative depth distribution between the near-surface and bulk regions the ratio between retention measured by TDS and that measured by IBA can be used. Fig. 7 presents the toroidal distributions of TDS/IBA ratio across both IWGL and WPL tiles. This toroidal dependence of the TDS/IBA ratio features a characteristic bell-curve shape with a significant increase from the periphery to the centre, i.e., from deposition zone to erosion zone. It should be noted that ILW1-3 results from the WPL are an exception and do not clearly follow this bell-curve behaviour; this can be attributed to the fact that of the TDS/IBA ratios in this tile are generally low (much lower than those for the IWGL) and therefore more susceptible to experimental scatter, which makes discerning a real coordinate dependence difficult in this case. A low TDS/IBA ratio describes a situation where a large fraction is retained in the near-surface region (indeed, if it is equal to one the entirety of retention occurs within the near-surface), while in the case of high TDS/IBA ratio a considerable, or even predominant, fraction is retained in the bulk.

It should be noted here that a non-negligible fraction of D retention occurs in the gaps of the castellated Be tile structure. According to [32], retention in the gaps can be comparable to that on plasma-facing side of the tiles. It could be argued that the results of TDS might overestimate the retention in the plasma-facing side by detecting content originating on the side surfaces of castellations used as experimental samples (i.e., surfaces in the gaps between castellations, not directly exposed to plasma). However, even assuming the worst case where the entirety of this D content is detected by the TDS, results from [32] suggest that this content can constitute at most ~50 % of the overall detected D. As TDS/IBA ratio considerably exceeds unity, particularly in the case of IWGL, even if retention measured by TDS was halved qualitatively the picture wouldn't change.

Comparing a single and three campaigns, as seen in Fig. 7a, there is a systematic increase of the TDS/IBA ratio in the erosion zone, while in the deposition zone values of TDS/IBA ratio are more comparable. This behaviour is particularly clear in the case of IWGL tiles. The increasing TDS/IBA ratio means that the relative fraction of D retained in the bulk compared to the near-surface region increases as a result of prior history of plasma exposure.

This conclusion is supported by comparing the D depth profiles measured by SIMS (Fig. 3) and inferred from NRA energy spectra (Fig. 4) in the deposition zone. Both techniques show a similar qualitative difference in the depth distribution of D content between ILW3 and ILW1-3. These results also indicate that near-surface D content is comparable between ILW3 and ILW1-3, while bulk content increases as a result of prior history of plasma exposure. It is notable that NRA energy spectra from the erosion zone present somewhat different picture, where there is a certain (though very low) D content very near the surface and then no content, detectable by NRA, beyond ~4 μm. This is in contradiction to the TDS results, which show considerable overall D content within erosion zone. To address this discrepancy, we must consider the origin of a bell-shaped curve in a toroidal distribution of the TDS/IBA ratio. It reflects the difference in the processes that primarily drive retention in different regions. In the deposition zone retention is primarily due to co-deposition, thus retained D tends to be accumulated near the surface, within the co-deposited layer. At the same time, in the erosion zone retention is primarily due to implantation and thus retained D can be driven by diffusion into the depth of material. Indeed, the driving force for diffusion is strongest in the erosion zone, as within a given tile both the ion flux and temperature are highest here. The fact that the NRA signal is very low indicates that volumetric concentration of D is low (below detection limit, estimated to be ~0.005 at. %), but at the same time TDS results indicate that overall amount of retained D is significant. This can be rationalized by assuming that this D was driven by diffusion to considerably larger depth than ~9 μm range of NRA. The diffusion depth, based on total D amount measured by TDS and bulk concentration below 0.005 % (NRA detection limit), can be estimated to be $\geq$ 50

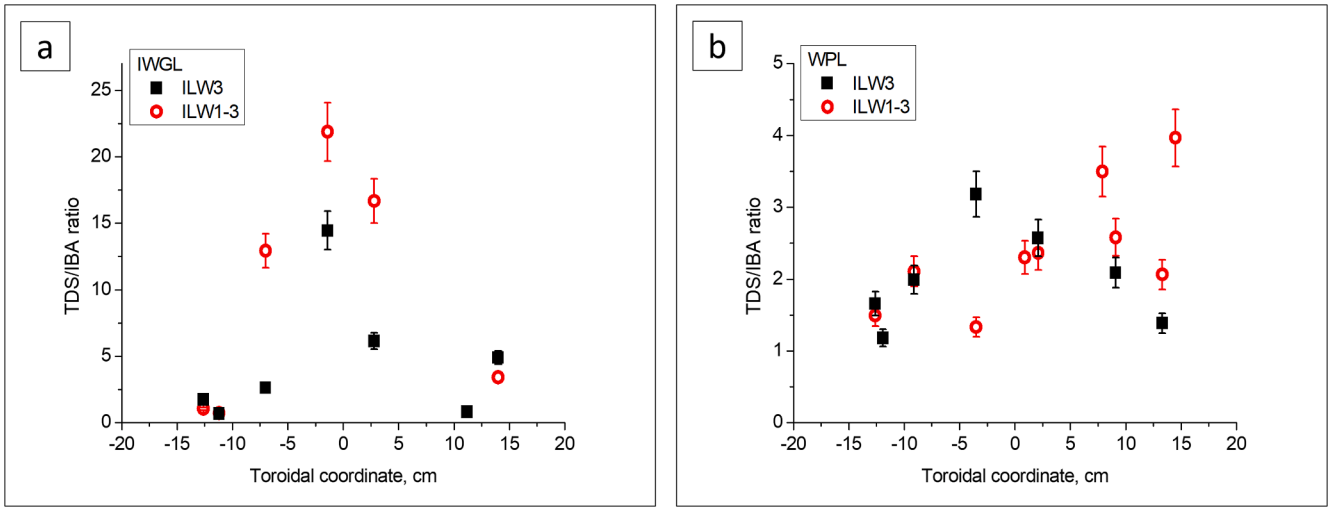

Fig. 7. Toroidal distribution of TDS/IBA retention ratio: (a) IWGL; (b) WPL. Note the difference in vertical scales between (a) and (b).

μm.In addition, the fact that both total retention measured by TDS, and TDS/IBA ratio increase in the erosion zone, indicates that as cumulative exposure time increases, diffusion front propagates ever deeper.

The observed changes in the shapes of desorption spectra – with the release peaks systematically shifting towards higher temperatures with the increase of exposure time – are also consistent with longer plasma exposure leading to the progressive increase in the contribution from the bulk region. Deuterium desorbed from larger depth would lead to the corresponding desorption peaks located at higher temperatures [33], which is exactly the experimentally observed behaviour.

To summarize, experimental evidence indicates that an increase in plasma exposure time leads to a non-linear increase of total retention where the near-surface D content is variable and dependent on recent conditions of plasma exposure, while bulk content progressively increases with time. Considering all the available data from different techniques, it can be suggested that the overall time dependence of retention in JET Be limiter components as observed by comparison of single and three campaigns, can be qualitatively described as being governed by diffusion. However, quantitatively the time dependence of retention does not appear to scale accordingly. According to the 2nd Fick's law, diffusion depth is proportional to $\sqrt{t}$, where t is diffusion time [34]. Assuming a diffusion-dominated regime, retention would scale proportionally to the diffusion depth, thus it would be proportional to $\sqrt{t}$ as well. As shown in Table 1, cumulative duration of the limiter phase on the IWGL for ILW1-3 is a factor ~6.6 longer than ILW3 alone, correspondingly $\sqrt{6.6} \approx 2.6$, compared to the difference in retention of 1.8. In the case of the WPL this difference is 1.6, correspondingly $\sqrt{1.6} \approx 1.3$, compared to the difference in retention of 1.4. This is an indication that depending on location with JET vessel, D accumulation as function of time scales with time at a somewhat slower rate than Fickian diffusion prediction. This could be partially attributed to the difference in temperature of the tiles that were in the vessel for one and three campaigns, as mentioned above. Another possible mechanism for this suppression of diffusion rate is the intervening series of protium plasma pulses at the end of ILW2. As mentioned earlier, it led to a fraction of D being lost from the near-surface region of limiter tiles, as measured by IBA. However, the fact that D content in the bulk of material is higher after three campaigns than after single campaign means that D has not been fully removed from the bulk regions and that despite this intervening cleaning operation (which ILW1-3 samples experienced and ILW3 ones didn't) cumulative retention was still increasing.

As a general remark it should be noted that during three ILW campaigns neutron production in JET plasmas was low, and therefore no significant formation of neutron-induced defects occurred. Observed retention behaviour is therefore governed by the intrinsic trapping and diffusion properties of Be. It can be expected that in the presence of significant amounts of neutron-induced damage retention behaviour will be different, however, present data obtained from available JET PFC samples do not allow to draw conclusions about such effects.

5. Conclusion

Deuterium retention was compared in the samples of JET ILW Be tiles that were in the JET vessel for the duration of a single (ILW3, 2015–2016) and three (ILW1-3, 2011–2016) campaigns, by means of TDS, IBA and SIMS. Comparison of samples from these tiles enabled the observation of D retention as function of plasma exposure time. It is demonstrated that total retention in ILW1-3 samples is higher than in equivalent ILW3 samples, which indicates that retention is not determined by the recent plasma exposure but is influenced by the prior exposure history, which in turn means that overall retention increases with cumulative time of exposure to plasma in the JET vessel. It is found that the retention scales non-linearly with the plasma exposure time. Instead, the increase in retention scales somewhat slower than the square root of time.

It is found that the dependence of D accumulation as a function of time in the near-surface region (within IBA range, ~9 μm) is different from that in the bulk. In the near-surface the D content appears to be strongly influenced by the recent conditions of plasma exposure. In contrast, in the bulk the D content progressively increases with plasma exposure time, and it is this increase of the bulk content that drives the increase of the overall retention with time.

Experimental findings are interpreted as the retention dynamics being governed by diffusion, and amount of retained D being proportional to the characteristic diffusion depth. The propagation of the diffusion front is slower than the 2nd Fick's law would predict. This is attributed to the fact that limiter tiles that were in the vessel for three campaigns, ILW1-3, experienced a period of wall cleaning by protium plasma, which removed a fraction of retained D, reducing therefore the available mobile D content and as a result slowing down inward diffusion away from plasma-exposed surface and into the bulk. As a consequence, as plasma exposure time increases, the relative contribution of the bulk increases as well. In addition, the increase of plasma exposure time leads to desorption peaks being systematically shifting to higher temperature, consistent with deeper diffusion.

These findings suggest that in the absence of hydrogen isotopes trapping on neutron-induced defects, retention in Be PFCs in the main chamber of fusion device will increase with time, with the relative contribution of bulk diffusion and desorption temperature both tending to increase. It is important to note that periodical fuel cleaning operations (such as using protium plasmas) that remove only part of the retained fuel do not stop this increase, only slow it down somewhat. This suggests that fuel removal becomes more difficult as exposure time increases, as removal techniques based on isotope exchange are more efficient in removal of hydrogen isotopes from the near-surface region [35], whilst temperature-based techniques such as baking can be expected to lose efficiency as well when desorption temperature is much higher than the permitted baking temperature [6].

CRediT authorship contribution statement

Y. Zayachuk: Writing – review & editing, Writing – original draft, Visualization, Validation, Resources, Project administration, Methodology, Investigation, Formal analysis, Data curation, Conceptualization. **N. Catarino:** Writing – review & editing, Validation, Resources, Methodology, Investigation. **J. Likonen:** Writing – review & editing, Validation, Resources, Methodology, Investigation. **M. Rubel:** Writing – review & editing, Validation, Investigation. **A. Widdowson:** Writing – review & editing, Validation, Investigation.

Declaration of competing interest

The authors declare that they have no known competing financial interests or personal relationships that could have appeared to influence the work reported in this paper.

Acknowledgements

This work has been carried out within the framework of the EUROfusion Consortium, funded by the European Union via the Euratom Research and Training Programme (Grant Agreement No 101052200 — EUROfusion). Views and opinions expressed are however those of the author(s) only and do not necessarily reflect those of the European Union or the European Commission. Neither the European Union nor the European Commission can be held responsible for them.

This work has been part-funded by the EPSRC Energy Programme (grant number EP/W006839/1). To obtain further information on the data and models underlying this paper please contact PublicationsManager@ukaea.uk.

The research used UKAEA's Materials Research Facility, which has been funded by and is part of the UK's National Nuclear User Facility and Henry Royce Institute for Advanced Materials.

Data availability

Data will be made available on request.

References

[1] G.F. Matthews, M. Beurskens, S. Brezinsek, M. Groth, E. Joffrin, A. Loving, M. Kear, M.-L. Mayoral, R. Neu, P. Prior, V. Riccardo, F. Rimini, M. Rubel, G. Sips, E. Villedieu, P. de Vries, M.L. Watkins, EFDA-JET contributors, JET ITER-like wall—overview and experimental programme, Phys. Scr. T145 (2011) 014001.

[2] C. Thomser, V. Bailescu, S. Brezinsek, J.W. Coenen, H. Greuner, T. Hirai, J. Linke, C.P. Lungu, H. Maier, G. Matthews, Ph. Mertens, R. Neu, V. Philipps,V. Riccardo, M. Rubel, C. Ruset, A. Schmidt, I. Uytdenhouwen, EFDA-JET contributors, Plasma Facing Materials for the JET ITER-Like Wall, Fusion Sci. Technol. 62 (2012).

[3] A. Widdowson, E. Alves, A. Baron-Wiechec, N.P. Barradas, N. Catarino, J.P. Coad, V. Corregidor, A. Garcia-Carrasco, K. Heinola, S. Koivuranta, S. Krat, A. Lahtinen, J. Likonen, M. Mayer, P. Petersson, M. Rubel, S. Van Boxel, J.E.T. Contributors, Overview of the JET ITER-like wall divertor, Nucl. Mater. Energy 12 (2017) 499–505.

[4] A. Widdowson, A. Baron-Wiechec, P. Batistoni, E. Belonohy, J.P. Coad, P. Dinca, D. Flammini, F. Fox, K. Heinola, I. Jepu, J. Likonen, S. Lilley, C.P. Lungu, G.F. Matthews, J. Naish, O. Pompilian, C. Porosnicu, M. Rubel, R. Villari, J.E.T. Contributors, Experience of handling beryllium, tritium and activated components from JET ITER like wall, Phys. Scr. T167 (2016) 014057.

[5] A. Baron-Wiechec, A. Widdowson, E. Alves, C.F. Ayres, N.P. Barradas, S. Brezinsek, J.P. Coad, N. Catarino, K. Heinola, J. Likonen, G.F. Matthews, M. Mayer, P. Petersson, M. Rubel, W. van Renterghem, I. Uytdenhouwen, JET-EFDA contributors, Global erosion and deposition patterns in JET with the ITER-like wall, J. Nucl. Mater. 463 (2015) 157–161.

[6] K. Heinola, A. Widdowson, J. Likonen, E. Alves, A. Baron-Wiechec, N. Barradas, S. Brezinsek, N. Catarino, P. Coad, S. Koivuranta, S. Krat, G.F. Matthews, M. Mayer, P. Petersson, J.E.T. Contributors, Phys. Scr. T167 (2016) 014075.

[7] K. Heinola, J. Likonen, T. Ahlgren, S. Brezinsek, G. De Temmerman, I. Jepu, G. F. Matthews, R.A. Pitts, A. Widdowson, J.E.T. Contributors, Nucl. Fusion 57 (2017) 086024.

[8] K. Heinola, A. Widdowson, J. Likonen, T. Ahlgren, E. Alves, C.F. Ayres, A. Baron-Wiechec, N. Barradas, S. Brezinsek, N. Catarino, P. Coad, C. Guillemaut, I. Jepu, S. Krat, A. Lahtinen, G.F. Matthews, M. Mayer, J.E.T. Contributors, Experience on divertor fuel retention after two ITER-Like Wall campaigns, Phys. Scr. T170 (2017) 014063.

[9] A. Baron-Wiechec, K. Heinola, J. Likonen, E. Alves, N. Catarino, J.P. Coad, V. Corregidor, I. Jepu, G.F. Matthews, A. Widdowson, Thermal desorption spectrometry of beryllium plasma facing tiles exposed in the JET tokamak, Fusion Eng. Des. 133 (2018) 135–141.

[10] L. Avotina, I. Jepu, A. Baron-Wiechec, M. Kresina, A., Widdowson and JET contributors, Thermal desorption of hydrogen isotopes from the JET Be plasma facing components, Phys. Scr. T171 (2020) 014009.

[11] S. Brezinsek, et al., Fuel retention studies with the ITER-Like Wall in JET, Nucl. Fusion 53 (2013) 083023.

[12] S. Brezinsek, JET-EFDA contributors, Plasma-surface interaction in the Be/W environment: Conclusions drawn from the JET-ILW for ITER, J. Nucl. Mater. 463 (2015) 11–21.

[13] T. Loarer, et al., Comparison of long term fuel retention in JET between carbon and the ITER-Like Wall, J. Nucl. Mater. 438 (2013) S108–S113.

[14] Y. Torikai, G. Kikuchi, A. Owada, S. Masuzaki, T. Otsuka, N. Ashikawa, M. Yajima, M. Tokitani, Y. Oya, S.E. Lee, Y. Hatano, N. Asakura, T. Hayashi, M. Oyaidzu, J. Likonen, A. Widdowson, M. Rubel, J.E.T. Contributors, Overview of tritium retention in divertor tiles and dust particles from the JET tokamak with the ITER-like wall, Nucl. Fusion 64 (2024) 016032.

[15] V. Philipps, T. Loarer, H.G. Esser, S. Vartanian, U. Kruezi, S. Brezinsek, G. Matthews, JET EFDA contributors, Dynamic fuel retention and release under ITER like wall conditions in JET, J. Nucl. Mater. 438 (2013) S1067–S1071.

[16] X. Litaudon, et al., Overview of the JET results in support to ITER, Nucl. Fusion 57 (2017) 102001.

[17] A. Widdowson, J.P. Coad, E. Alves, A. Baron-Wiechec, N.P. Barradas, S. Brezinsek, N. Catarino, V. Corregidor, K. Heinola, S. Koivuranta, S. Krat, A. Lahtinen, J. Likonen, G.F. Matthews, M. Mayer, P. Petersson, M. Rubel, J.E.T. Contributors, Overview of fuel inventory in JET with the ITER-like wall, Nucl. Fusion 57 (2017) 086045.

[18] A. Widdowson, S. Aleiferis, E. Alves, L. Avotina, A. Baron-Wiechec, N. Catarino, J. P. Coad, V. Corregidor, K. Heinola, I. Jepu, C. Makepeace, J.E.T. Contributors, Fuel inventory and material migration of JET main chamber plasma facing components compared over three operational periods, Phys. Scr. T171 (2020) 014051.

[19] Y. Oya, S. Masuzaki, M. Tokitani, M. Nakata, F. Sun, M. Oyaidzu, K. Isobe, N. Asakura, T. Otsuka, A. Widdowson, J. Likonen, M. Rubel, J.E.T. Contributors, Comparison of hydrogen isotope retention in divertor tiles of JET with the ITER-Like Wall following campaigns in 2011–2012 and 2015–2016, Fusion Sci. Technol. 76 (4) (2020) 439–445.

[20] A. Lahtinen, J. Likonen, S. Koivuranta, A. Hakola, K. Heinol, C.F. Ayres, A. Baron-Wiechec, J.P. Coad, A. Widdowson, J. Räisänen, J.E.T. Contributors, Deuterium retention in the divertor tiles of JET ITER-Like wall, Nucl. Mater. Energy 12 (2017) 655–661.

[21] C. Makepeace, C. Pardanaud, P. Roubin, I. Borodkina, C. Ayres, P. Coad, A. Baron-Wiechec, I. Jepu, K. Heinola, A. Widdowson, S. Lozano-Perez, J.E.T. Contributors, The effect of beryllium oxide on retention in JET ITER-like wall tiles, Nucl. Mater. Energy 19 (2019) 346–351.

[22] M. Faitsch, T. Eich, B. Sieglin, J.E.T. Contributors, Correlation between near scrape-off layer power fall-off length and confinement properties in JET operated with carbon and ITER-like wall, Plasma Phys. Controlled Fusion 62 (2020) 085004.

[23] G. Federici, C.H. Skinner, J.N. Brooks, J.P. Coad, C. Grisolia, A.A. Haasz, A. Hassanein, V. Philipps, C.S. Pitcher, J. Roth, Plasma-material interactions in current tokamaks and their implications for next step fusion reactors, Nucl. Fusion 41 (2001) 1967–2137.

[24] R. Arredondo, K. Schmid, F. Subba, G.A. Spagnuolo, Preliminary estimates of tritium permeation and retention in the first wall of DEMO due to ion bombardment, Nucl. Mater. Energy 28 (2021) 101039.

[25] E. Pajuste, A.S. Teimane, G. Kizane, L. Avotina, M. Halitovs, A. Lescinskis, A. Vitins, P. Kalnina, E. Lagzdina, R.J. Zabolockis, J.E.T. Contributors, Tritium in plasma-facing components of JET with the ITER-Like-Wall, Phys. Scr. 96 (2021) 124050.

[26] C.F. Maggi, JET contributors, Overview of T and D-T results in JET with ITER-like Wall, Nucl. Fusion 64 (2024) 112012.

[27] Y. Zayachuk, I. Jepu, M. Zlobinski, C. Porosnicu, N. Catarino, E. Pajuste, P. Petersson, L. Dittrich, J.P. Coad, E. Grigore, C. Postolache, E. Alves, G. Kizane, M. Rubel, A. Widdowson, Nucl. Fusion 63 (2023) 096010.

[28] N.P. Barradas, C. Jeynes, Advanced physics and algorithms in the IBA DataFurnace, Nuclear Instrum. Methods Phys. Res. B 266 (2008) 1875–1879.

[29] W. Möller, F. Besenbacher, A note on the 3He + D nuclear-reaction cross section, Nucl. Inst. Methods 168 (1980) 111–114.

[30] J.F. Ziegler, M.D. Ziegler, J.P. Biersack, SRIM - The stopping and range of ions in matter, Nucl. Instrum. Meth. B 268 (2010) 1818–1823.

[31] G. Arnoux, I. Balboa, M. Clever, S. Devaux, P. De Vries, T. Eich, M. Firdaouss, S. Jachmich, M. Lehnen, P.J. Lomas, G.F. Matthews, I. Ph Mertens, V.R. Nunes, C. Ruset, B. Sieglin, D.F. Valcárcel, J. Wilson, K.-D. Zastrow, JET-EFDA contributors, Power handling of the JET ITER-like wall, Phys. Scr. T159 (2014) 014009.

[32] M. Rubel, P. Petersson, Y. Zhou, J.P. Coad, C. Lungu, I. Jepu, C. Porosnicu, D. Matveev, S. Brezinsek, A. Widdowson, E., Alves and JET contributors, Fuel inventory and deposition in castellated structures of JET-ILW, Nucl. Fusion 57 (2017) 066027.

[33] Y. Zayachuk, M.H.J. 't Hoen, I. Uytdenhouwen, G. Van Oost, Thermal Desorption Spectroscopy of W–ta Alloys, Exposed to High-Flux Deuterium Plasma, Phys. Scr. T145 (2011) 014041.

[34] R.M. Barrer, Diffusion in and through solids, Cambridge University Press, 1951.

[35] D. Matveev, D. Douai, T. Wauters, A. Widdowson, I. Jepu, M. Maslov, S. Brezinsek, T. Dittmar, I. Monakhov, P. Jacquet, P. Dumortier, H. Sheikh, R. Felton, C. Lowry, D. Ciric, J. Banks, R. Buckingham, H. Weisen, L. Laguardia, G. Gervasini, E. de la Cal, E. Delabie, Z. Ghani, J. Gaspar, J. Romazanov, M. Groth, H. Kumpulainen, J. Karhunen, S. Knipe, S. Aleiferis, T. Loarer, A. Meigs, C. Noble, G. Papadopoulos, E. Pawelec, S. Romanelli, S. Silburn, E. Joffrin, E. Tsitrone, F. Rimini, C.F. Maggi, J. E.T. Contributors, Tritium removal from JET-ILW after T and D–T experimental campaigns, Nucl. Fusion 63 (2023) 112014.